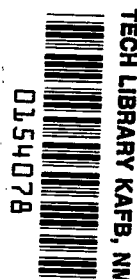


NASA TECHNICAL NOTE



NASA TN D-1865

NASA TN D-1865



INVESTIGATION OF AIR DAMPING OF CIRCULAR AND RECTANGULAR PLATES, A CYLINDER, AND A SPHERE

by David G. Stephens and Maurice A. Scavullo

Langley Research Center

Langley Station, Hampton, Va.



INVESTIGATION OF AIR DAMPING
OF CIRCULAR AND RECTANGULAR PLATES,
A CYLINDER, AND A SPHERE

By David G. Stephens and Maurice A. Scavullo

Langley Research Center
Langley Station, Hampton, Va.

NATIONAL AERONAUTICS AND SPACE ADMINISTRATION

For sale by the Office of Technical Services, Department of Commerce,
Washington, D.C. 20230 -- Price \$1.00

INVESTIGATION OF AIR DAMPING
OF CIRCULAR AND RECTANGULAR PLATES,
A CYLINDER, AND A SPHERE

By David G. Stephens and Maurice A. Scavullo
Langley Research Center

SUMMARY

An investigation was conducted to determine the mechanism of air damping exhibited by rigid bodies of different shapes oscillating in a pressure environment. Circular and rectangular plates, as well as a sphere and cylinder, were attached to cantilever springs and the free decay of an induced oscillation was measured at pressure levels from atmospheric to 4×10^{-2} torr. Data are presented to show the effect of pressure, vibratory amplitude, frequency, shape, and surface area on the air damping of the models. Results indicate that the magnitude of the air damping may greatly exceed the structural damping of the system. The air damping associated with the plates is directly proportional to the pressure and amplitude and is indicative of dissipative loads proportional to the dynamic pressure. Furthermore, the plate damping was found to be independent of shape and is a nonlinear function of the surface area. The sphere and cylinder exhibit viscous damping characteristics which are in good agreement with available theory.

INTRODUCTION

The vibratory response of a mechanical system is highly dependent upon the total damping. In most situations this damping results from the action of several dissimilar dissipative mechanisms, one or more of which may be a function of the operating environment. Some of the more common sources of energy dissipation include internal hysteresis (ref. 1), interface or joint friction (ref. 2), and external or air damping. The air damping is dependent upon the magnitude of the pressure environment and, therefore, deserves particular attention in studying the response of systems designed to operate throughout a wide range of pressure or density. If, for example, the vibration tests of a space vehicle are conducted under atmospheric pressure conditions, the damping level and consequently the response will be somewhat different than in the actual operating environment which involves reduced pressures. Thus the interpretation and extrapolation of the results of such tests must include the effects of the pressure environment.

An object moving in a fluid such as air may lose energy to the surrounding medium as a result of one or more resistive effects. The dissipation may result from viscous laminar boundary-layer friction, sound radiation, and vortex formation and shedding. However, the relative importance of each of these phenomena on the damping of a vibrating body is not known. Results of previous investigations are limited to the effects of a single loss phenomenon on the damping of specific objects. For example, theoretical studies of the viscous damping forces experienced by a sphere and cylinder oscillating in a fluid are discussed by Lamb (ref. 3) and by Stokes (ref. 4), respectively. When these objects are undergoing relatively low frequency oscillations, theory predicts that they will experience forces proportional to the velocity and the square root of the fluid density. These predictions were examined experimentally in reference 5 in which a cylinder was swung as a pendulum about one end and limited damping measurements taken at several pressure levels. For the frequency examined (0.7 cps), good agreement was found with the theory. The damping of a "two-dimensional" plate resulting from sound radiation is discussed in references 6 and 7. A rigid plate oscillating such that the fluid cannot pass over the edges is theoretically shown to experience damping forces directly proportional to the density, velocity, and the square of the area although no experimental verification is indicated. A case in which vortex effects may have been predominant is discussed in reference 8. The air damping force experienced by a small cantilever beam is shown to be proportional to the square of the vibratory velocity.

The purpose of this paper is to present the results of an investigation of the characteristics of the air damping exhibited by rigid circular and rectangular plates, a sphere, and a cylinder oscillating in a pressure environment varying from atmospheric to 4×10^{-2} torr. The effects of area, shape, vibratory amplitude, excitation frequency, and pressure are examined.

SYMBOLS

A	area of a panel, sq ft
a	radius of sphere, cylinder, or disk, ft
b	velocity squared damping coefficient, $\frac{\text{lb-sec}^2}{\text{sq ft}}$
c	viscous damping coefficient, $\frac{\text{lb-sec}}{\text{ft}}$
E	energy of oscillating system, lb-ft
ΔE	energy dissipated per cycle, lb-ft
f	frequency of oscillation, $\frac{\text{cycles}}{\text{sec}}$

k	slope, ft^2 (see fig. 8)
l	length of plate or cylinder, ft
m	vibratory mass, $\frac{\text{lb-sec}^2}{\text{ft}}$
p	pressure of chamber, torr
t	thickness of material, ft
u	vibratory velocity, ft/sec
w	width of plate, ft
X	damping force, lb
y	vibratory amplitude, ft
β	$= \left(\frac{\omega}{2\nu} \right)^{1/2}, \frac{1}{\text{ft}}$
δ	logarithmic decrement, $\frac{1}{n} \log \frac{y_0}{y_n}$
ρ	fluid density, $\frac{\text{lb-sec}^2}{\text{ft}^4}$
ν	kinematic viscosity, $\frac{\text{ft}^2}{\text{sec}}$
ω	circular frequency of oscillations, $\frac{\text{radians}}{\text{sec}}$

Subscripts:

a	air
e	external
i	internal
j	joint
n	nth cycle of vibration
o	initial cycle of vibration
t	beam tip

x extraneous damping
 1,2 designates cycle
 max maximum

Dots over symbols denote derivatives with respect to time.

APPARATUS AND TEST PROCEDURE

Vacuum Equipment

The vacuum system used in this investigation is shown schematically in figure 1. The chamber consisted of a glass bell jar 18 inches in diameter and 30 inches high which was sealed to a 6-inch steel spacer. The steel spacer provided access ports (for electronic leads and vacuum lines) from the side rather than from the bottom of the chamber as in a conventional bell jar system. The spacer was in turn mounted on a steel base plate; and the system was anchored to a massive steel and concrete block to eliminate the transmission of vibratory energy from the apparatus to the adjoining structure. A 5-cubic-foot-per-minute mechanical pump was used to obtain the desired pressure levels between the limits of 1 atmosphere and 4×10^{-2} torr. A flexible coupling between the pump and the chamber reduced the transmission of pump vibrations to the system.

Vibration Equipment

The equipment used to study the damping of the various models within the vacuum chamber is shown schematically in figure 2. Depending upon the desired frequency, one of two cantilever beams was employed to support the models and provide the oscillation. The beams, $15\frac{1}{4}$ inches long and $1\frac{1}{2}$ inch wide, had thicknesses of $1\frac{1}{8}$ and $3\frac{3}{8}$ inch and were tuned to frequencies of 3.8 and

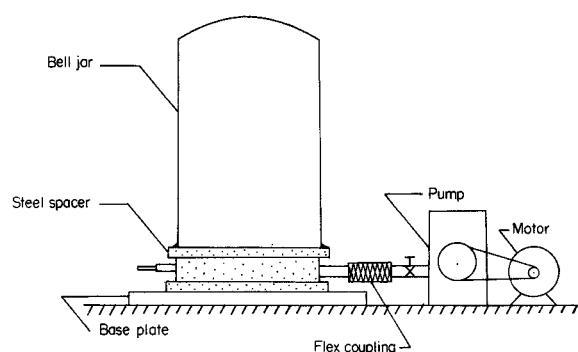


Figure 1.- Schematic of vacuum system.

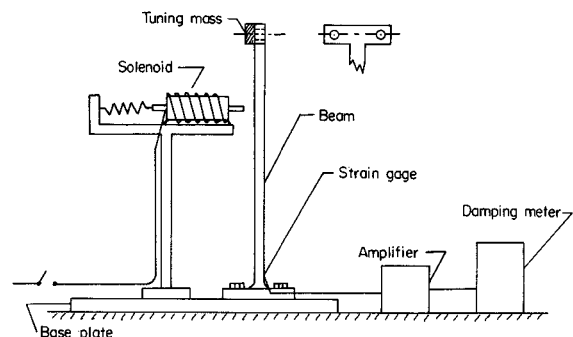


Figure 2.- Test apparatus and instrumentation.

21.2 cps, respectively, by attaching a small mass to the beam tip. Each beam, machined from a single piece of stainless steel, had a relatively large foot for mounting the assembly to the base plate and a T-section at the tip for attaching the models. A spring-loaded solenoid was used to excite the fundamental vibratory mode of the cantilever beam. When energized the solenoid slug moved forward and imparted a static deflection to the beam. Upon de-energizing, the slug was quickly retracted by the spring and the free decay of the model-beam system was studied.

In addition to these beams, an aluminum beam $25\frac{3}{4}$ inches \times 2 inches \times $\frac{1}{2}$ inch was used to study the damping characteristics of three large plates at a frequency of 3.8 cps. Since this study was conducted under atmospheric pressure conditions, the beam was deflected and released manually.

Instrumentation

The damped oscillations of the model-beam system were monitored by means of a strain gage attached near the root of the beam. The output of this gage was amplified and fed into an electronic dampometer which measured the frequency and logarithmic decrement of the oscillation.

A Bourdon gage and an ion gage were used to measure the pressure in the bell jar. The Bourdon gage was used from a pressure of 1 atmosphere to 1 torr and the ion gage was used from 1 torr to the lowest attainable pressure in the system (4×10^{-2} torr).

Models

The damping was studied for the models shown and described in table I. The plates with surface areas of 15, 30, and 45 square inches and the sphere and cylinder, each having a projected surface area of 30 square inches, were used for most of the tests. These models were selected to examine the effects of shape and area on the air damping within the vacuum system. The rectangular plates having surface areas between 12 and 39 square inches were used in limited tests to better define the damping-area relationship. The remaining rectangular plates, having surface areas of 93.8, 152, and 240 square inches, were studied at atmospheric conditions to investigate the possibility of applying the results obtained for the small models to larger systems. The materials, from which the models were constructed, are given in table I and were chosen to maintain approximately the same weight for all models used in a particular test. All panels were machined with square edges.

Test Procedure

The damping characteristics of the beams alone, tuned to 3.8 or 21.2 cps by the addition of concentrated masses to the tip, were studied initially. The selected model was then securely attached to the tip of the beam and damping of

the assembled system, tuned in a similar manner to a frequency of either 3.8 or 21.2 cps, was measured. The basic procedure for measuring this damping within the vacuum chamber was essentially the same for each case. The chamber was pumped down to the desired pressure level and for all but the lowest pressure level (4×10^{-2} torr) the pump was stopped while the test points were taken. The beam was deflected by means of the solenoid and released. When the amplitude of the ensuing oscillation reached a pre-selected value, the output of the strain gage triggered the dampometer which measured the decay of the oscillation until the amplitude reached 7/10 of the value for the initial reading. The damping in terms of the log decrement was then calculated from

$$\delta = \frac{1}{n} \log \frac{y_0}{y_n} = \frac{1}{n} \log \frac{10}{7}$$

where n was the number of cycles recorded between these amplitude limits. In all cases the initial deflection was of sufficient amplitude to allow any undesirable transients to decay before a test point was taken.

The decrement was measured at various positions along the envelope to determine the dependency, if any, of the damping on the amplitude. The amplitude associated with a test point was determined in a separate test in which the dynamic deflection of the system was measured at the selected output levels. The deflection, at various positions along the beam and model, was determined by placing a stylus at the desired position and measuring the resulting trace. For the amplitude range considered, the normalized mode shape of the tuned beam was found to be independent of amplitude and the same for each assembly at a given frequency.

In limited tests conducted to examine extrapolation techniques, panels of considerably larger area were examined for several amplitudes at atmospheric pressure only, as size precluded installation in the vacuum system. The procedure was essentially the same. The damping of the beam, tuned to the frequency of the beam panel assembly (3.8 cps), was studied and then the total damping of the beam-panel system was examined.

ANALYSIS

The test program and subsequent data reduction were directed toward the examination of the effects of pressure or density, amplitude, frequency, shape, and area on the air damping of the models. An investigation of the free decay of the system was found to be most expedient for measuring the damping and isolating the effects of the variables. The decay of the oscillation was analyzed over selected portions of the envelope and specified in terms of logarithmic decrement δ . For purposes of this investigation, the decrement is physically interpreted as the ratio of the energy lost per cycle to twice the total energy and is given by the equation

$$\delta = \frac{\Delta E}{2E} \quad (1)$$

as is discussed in reference 9. Two characteristics of equation (1) should be noted. First, the relationship is applicable for analyzing or interpreting any damped oscillation regardless of the type of decay (viscous, velocity squared, and so forth); that is, no assumption is made as to the shape of the envelope. This effect can be seen by considering a hypothetical case in which an arbitrary velocity time history is available. Application of equation (1) yields

$$\delta = \frac{\Delta E}{2E} = \frac{\frac{1}{2} m (u_{\max,1}^2 - u_{\max,2}^2)}{m \left(\frac{u_{\max,1} + u_{\max,2}}{2} \right)^2} \quad (2)$$

where ΔE is the change in kinetic energy between successive peaks and E represents the average of peak energy levels of the system, m is the mass of the system, and u_{\max} is the maximum velocity. Equation (2) reduces to

$$\frac{\Delta E}{2E} = 2 \left(\frac{\frac{u_{\max,1}}{u_{\max,2}} - 1}{\frac{u_{\max,1}}{u_{\max,2}} + 1} \right) \quad (3)$$

This relationship is the first term in the series expansion of $\log \frac{u_{\max,1}}{u_{\max,2}}$

which is by definition the log decrement. The error in assuming that $\delta = \frac{\Delta E}{2E}$ is that involved in dropping the higher ordered terms of the series which are usually very small. The second point to be noted is the additive nature of the various sources of damping. For example, if the energy loss is attributed to the combination of internal dissipation, joint losses, and external losses, then the decrement can be written as

$$\delta = \frac{\Delta E}{2E} = \frac{\Delta E_i + \Delta E_j + \Delta E_e}{2E} \quad (4)$$

where ΔE_i represents the internal losses; ΔE_j , the joint losses; and ΔE_e , the external losses. Thus, if the losses attributed to one or more sources are known, these losses can be subtracted from the total measured decrement to yield a value for the remaining energy dissipation.

For the configurations under study, the total decrement was measured throughout a wide range of variables. The decrement was written as

$$\delta = \frac{\Delta E_x + \Delta E_a}{2E} \quad (5)$$

where ΔE_x is the total of all the extraneous damping of the beam system such as the internal hysteresis of the beam, dissipation at the beam support interface, and so forth. The value of ΔE_x was accurately determined prior to testing a particular configuration by tuning the beam alone to the desired frequency and measuring the decrement. The additional damping measured for the assembled system was isolated and attributed to the air resistance of the models and can be written as

$$\delta_a = \frac{\Delta E_a}{2E} \quad (6)$$

Once the air damping of the models was isolated, examination of the effects of each of the variables (pressure or density, amplitude, frequency, area, and shape) on the decrement or more specifically the energy loss per cycle ΔE remained. In this case the loss per cycle is equal to the work done by the dissipative force or

$$\Delta E = \int_c |X \, dy| \quad (7)$$

If, for example, the forces are viscous or directly proportional but opposed to velocity as discussed in reference 8, the energy loss would be

$$\Delta E = \int_c |X \, dy| = \int_c |c \dot{y} \, dy| \quad (8)$$

where c may be a function of the density, area, and so forth, but independent of velocity \dot{y} . Since the motion of the models is essentially harmonic, the velocity is assumed to be

$$\dot{y} = y_o \omega \cos \omega t \quad (9)$$

for the case of low damping. Hence

$$\Delta E = \int_0^{2\pi/\omega} c y_o^2 \omega^2 \cos^2 \omega t \, dt \quad (10)$$

which when integrated gives

$$\Delta E = c y_o^2 \omega \pi \quad (11)$$

The corresponding total energy or E is simply

$$E = \frac{1}{2} m y_o^2 \omega^2 \quad (12)$$

and hence

$$\delta = \frac{\pi c}{m\omega} \quad (13)$$

where m is the oscillatory mass, and ω is the circular frequency. Thus in the viscous case the decrement is independent of amplitude but is a function of frequency.

If the damping is proportional to the velocity squared, a similar calculation in which

$$\Delta E = \int_c \left| b \dot{y}^2 dy \right| = b y_o^3 \omega^3 \int_0^{2\pi/\omega} \left| \cos^3 \omega t \right| dt \quad (14)$$

will yield a decrement

$$\delta = \frac{8}{3} \frac{b y_o}{m} \quad (15)$$

which is a linear function of displacement and independent of frequency for a particular system.

When the data were analyzed and presented, the effects of pressure and amplitude were isolated to determine, for a particular system, whether the damping was viscous, velocity squared, or of some intermediate form. The data were then presented in forms suggested by either equation (13) or (15) to determine the relationships between pressure, area, shape, frequency, and damping.

In the case of the sphere or cylinder, equations are available for comparison of the experimental results with theory. The problem of a sphere performing pendulum oscillations of small amplitude in an incompressible infinite mass of viscous fluid has been treated by Lamb and Stokes, references 3 and 4, respectively. The derivation of the resultant force acting on the spherical surface yields a force component which is linearly proportional to and in opposition to the velocity as follows:

$$X = 3\pi\rho a^3\omega\left(\frac{1}{\beta a} + \frac{1}{\beta^2 a^2}\right)u \quad (16)$$

where

X	damping force
ρ	fluid density
a	radius of sphere
ω	circular frequency of oscillations

$$\beta = (\omega/2\nu)^{1/2}$$

ν kinematic viscosity

u velocity

Using

$$\delta = \frac{\pi c}{m\omega} = \frac{\pi}{m\omega} \left(\frac{X}{u} \right)$$

where

c damping coefficient

m oscillatory mass

Hence the logarithmic decrement is

$$\delta = \frac{3\pi^2 \rho a^3 \left(\frac{1}{\beta a} + \frac{1}{\beta^2 a^2} \right)}{m} \quad (17)$$

The viscous damping force on a cylinder with a high length-radius ratio vibrating rectilinearly normal to its length at small amplitudes has been calculated by Stokes. (See ref. 4.) The damping force is given as

$$X = \pi a^2 \rho l \omega \left(\frac{2}{\beta a} + \frac{1}{\beta^2 a^2} \right) u \quad (18)$$

where a and l are the radius and length of the cylinder, respectively, and the other symbols are as previously defined.

Again setting

$$\delta = \frac{\pi c}{m\omega} = \frac{\pi}{m\omega} \left(\frac{X}{u} \right)$$

yields

$$\delta = \frac{\pi^2 a^2 \rho l}{m} \left(\frac{2}{\beta a} + \frac{1}{\beta^2 a^2} \right) \quad (19)$$

PRESENTATION AND DISCUSSION OF RESULTS

The primary objective of the test program was the isolation and examination of the effect of density on the air damping of the two- and three-dimensional shapes. This objective was accomplished by examining the

difference in magnitude of the total system damping and the beam damping measured over a wide range of pressures. At each pressure level, the damping was measured for several amplitudes of vibration so the effect of amplitude could also be isolated and studied. By comparing the data from each of the systems, the effects of frequency, shape, and area become evident. The relationships established by these data were compared with the measured damping of panels of much larger area to examine the validity of extrapolation. The data which follow exemplify these points.

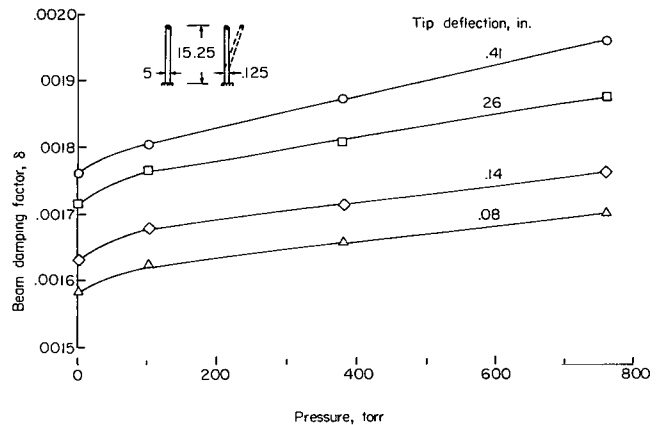


Figure 3.- Variation of beam damping with pressure. $f = 3.8$ cps.

Beam Damping

The damping associated with the fundamental mode of oscillation of the cantilever beam, tuned to 3.8 cycles per second, is presented in figure 3. These data served as a tare for obtaining the air damping of the low-frequency assemblies and similar results for the beam tuned to 21.2 cycles per second were used in the high-frequency cases. The damping factors, in terms of the logarithmic decrement δ , are shown as a function of the pressure for several different tip amplitudes (note suppressed zero). In this case, as well as those to follow, the data points represent an average of five or more measured values. The total damping associated with the beam exhibits a near-linear dependency on pressure in the range between atmospheric pressure and 100 torr. Below 100 torr the damping factors deviate from this linear pressure relationship and approach values at 4×10^{-2} torr which are most probably due to the internal hysteresis and joint friction. No attempt was made to isolate these particular effects as the results served only as a tare. At all pressures the magnitude of the damping is proportional to the tip amplitude. The curve as presented was rerun periodically and was found to be highly repeatable.

Total Damping of Beam-Model System

A typical sample of the data, as recorded, is shown in figure 4 to illustrate the relative magnitudes of the beam and total damping. The total damping recorded for the 30-square-inch rectangle mounted on the tip of the low-frequency beam is presented as a function of pressure

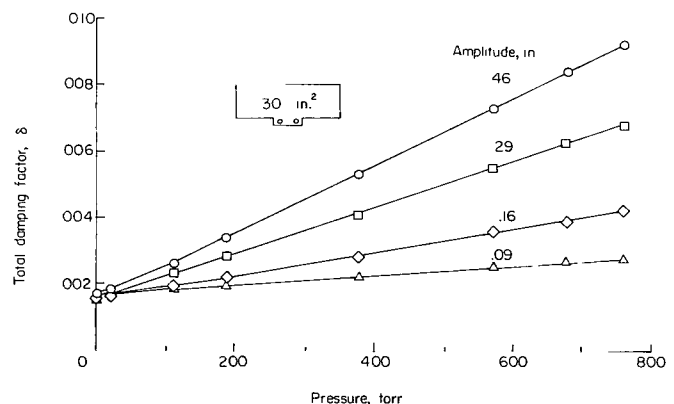
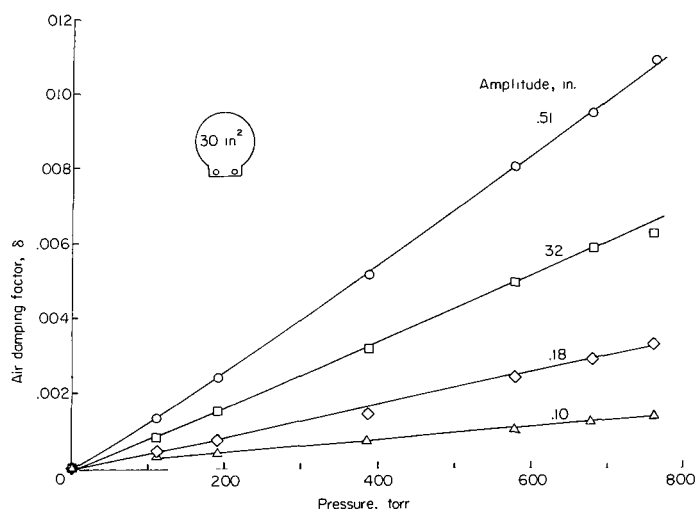
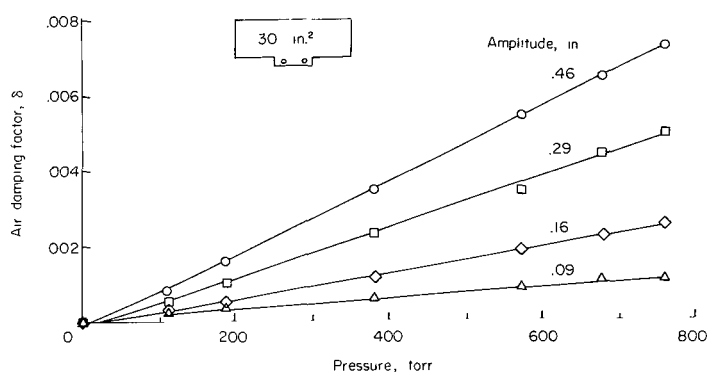


Figure 4.- Variation of total damping with pressure. $f = 3.8$ cps.

and amplitude. The amplitudes refer to the average deflection of the center of the plate during the damping measurement and correspond to the beam tip deflections shown in the previous figure. It is interesting to note the significant increase in the system damping with the addition of the plate. For example, an increase in damping by a factor of approximately five is noted in the high-pressure region. As the pressure is decreased, the values of damping converge to the values measured for the beam alone in the low-pressure region. This condition indicates that no extraneous damping is introduced into the system with the addition of the plate and thus the additional damping may be attributed to the air resistance.



(a) 30-square-inch disk.



(b) 30-square-inch rectangle.

Figure 5.- Variation of air damping with pressure. $f = 3.8$ cps.

A separate test was conducted to determine the effect, if any, of the bell jar on the damping. A 45-square-inch plate was attached to the beam (3.8 cps) and the damping recorded of several amplitudes at atmospheric pressure. The bell jar was then removed and the test rerun. Since the data obtained with and without the bell jar were essentially identical, it was concluded that the presence of the bell jar per se had no significant effect on the damping of the models.

Damping of Two-Dimensional Models

Effect of pressure.- The dependency of the air damping on the pressure, and hence on the density of the test medium, is presented in figure 5. The air damping, obtained by subtracting the beam damping from the total damping at corresponding pressures and amplitudes, is shown for the 30-square-inch plates at 3.8 cps. The damping factor exhibits a linear dependency on the pressure throughout the range examined. A strong dependency of the damping on the amplitude of deflection is also noted and indicates the presence of a non-linear damping phenomena. Identical trends were noted in the

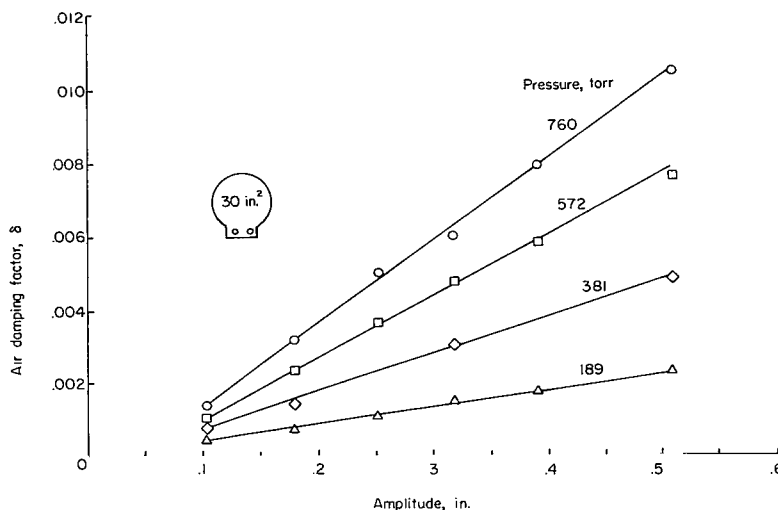
case of the 15- and 45-square-inch plates and these results are presented in a subsequent section on shape in which all the data are compared.

Effect of amplitude.-

The variation of damping with amplitude for the two 30-square-inch configurations is presented in figure 6. The trends existing in these cases are again representative of the results obtained for the other plates studied at 3.8 cps. For the range of amplitude examined, the damping is a near-linear function of plate deflection.

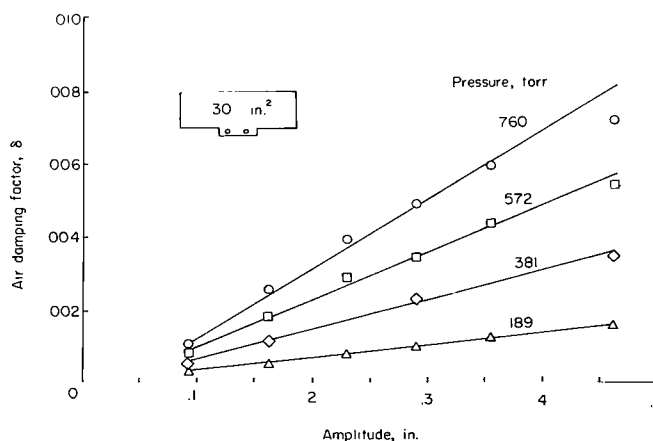
Because of this linear dependency, the damping is apparently of the velocity squared type as previously discussed. Thus, the resistance force is proportional to the dynamic pressure $\frac{1}{2}\rho u^2$ as would be found in the case of a panel immersed in a steady stream of incompressible fluid. It should be noted that an extension of the faired lines will not intersect the origin. It is possible that in the low-amplitude range, the forces become viscous in nature and therefore the amplitude dependency or slope of the curve is reduced.

Effect of frequency.- The effects of frequency on the damping-pressure-amplitude relationship observed in the previous cases were examined by employing the beam having a tuned frequency of 21.2 cps. The decrements are presented in figure 7 as a function of pressure and amplitude for the 30-square-inch disk. Except in the very low pressure region, the damping is again a linear function of pressure as shown in figure 7(a). Because of the beam stiffness, amplitudes comparable to those of the low-frequency case could not be obtained with the solenoid. Consequently, the effect of amplitude on the air damping was examined by removing the bell jar and displacing the beam manually.



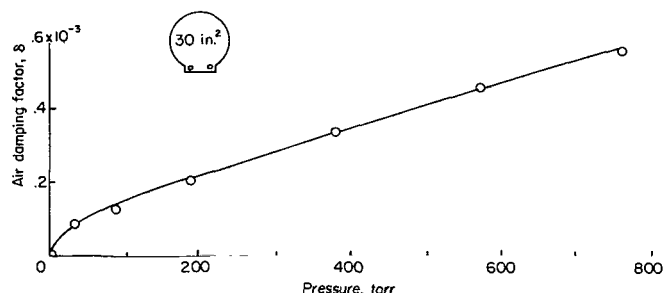
(a) 30-square-inch disk.

Figure 6.- Variation of air damping with amplitude.
f = 3.8 cps.

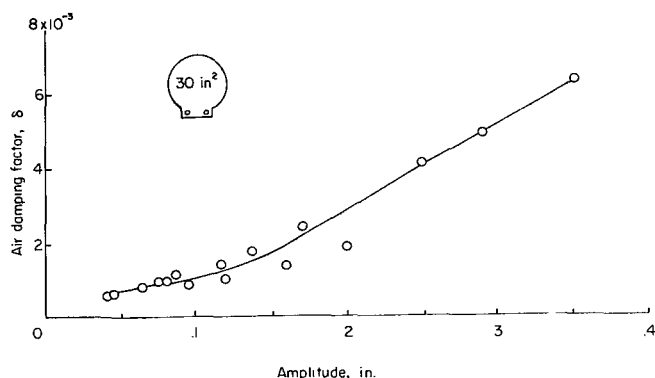


(b) 30-square-inch rectangle.

Figure 6.- Concluded.



(a) Variation of air damping with pressure. Amplitude 0.44 in.



(b) Variation of air damping with amplitude. Pressure 760 torr.

Figure 7.- Variation of air damping with pressure and amplitude. $f = 21.2$ cps.

In the region of higher amplitudes, the damping is again directly proportional to displacement as shown in figure 7(b). As the amplitude is decreased, however, the damping becomes less dependent upon amplitude as was found in the low-frequency case.

Effect of shape.- The effects of plate shape were examined by comparing the damping factors associated with the circular and rectangular plates. The decrements, measured over a wide range of pressure and amplitude while attached to the beam of lower frequency, are summarized in figure 8. The log decrement δ is presented as a function of the parameter $\rho y/m$ where ρ is the density of the air within the chamber, y is the amplitude of the center of the plate, and m is the effective mass of the system located at the center of the plate. The symbols indicate the pressure levels at which the measurements were taken. The decrement is a linear function of the parameter $\rho y/m$ which is indicative of velocity squared damping. For a given area, $\delta = k\rho y/m$ where k is the slope of the curve associated

with that particular area. When the results for the circular and rectangular plates are compared the values of k are seen to be independent of shape but are highly dependent upon the area.

Effect of area.- A detailed examination of the nonlinear dependency of the air damping on plate area necessitated the use of the additional plates of surface areas between 12 and 39 square inches. The results of this examination are shown in figure 9. The measured decrement is presented as a function of plate area for two particular amplitudes at each frequency. The functional dependency was found to be $\delta \approx A^{4/3}$, the exponent $4/3$ being determined from the slopes of the four curves. It is interesting to note that the dependency on area is greater than that experienced by a similar plate in a steady flow field but less than the A^2 relationship discussed in reference 6 for sound radiation damping.

These results, obtained at atmospheric pressure, are compared with all the low-frequency data previously summarized. (See fig. 8.) As previously found, the decrement δ is a linear function of $\rho y/m$ for a particular area

but the slope $\delta m/\rho y$ did not vary directly with area. Thus for comparison purposes, all the low-frequency data are presented in figure 10 where the parameter $\delta m/\rho y$ is shown as a function of area. The atmospheric data of figure 9 are represented by the circles and the data from figure 8 (slopes) are shown by the squares. The results indicate that the decrement

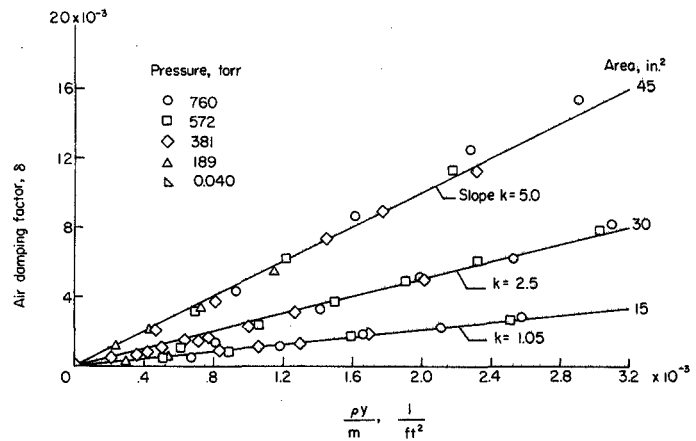
$$\delta = 22 \frac{\rho y A^{4/3}}{m} \quad \text{for all the low-}$$

frequency data. In the case of the high-frequency data, the same relationship is adequate for predicting the damping for amplitudes greater than

0.15 inch. Below 0.15 inch, the damping ceases to be a linear function of amplitude and therefore cannot be represented by the empirical relationship.

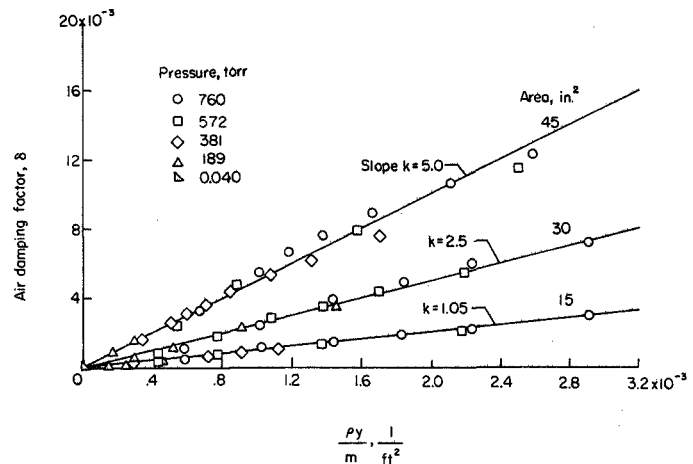
The application of the relationship developed in the previous section to plates of large area was examined. Plate areas of 71.3, 128, and 220 square inches (plate area minus area of beam overlay) were selected to provide an order-of-magnitude variation in size. The decrements measured at atmospheric pressure for three amplitudes are shown in figure 11 and are seen to be in excellent agreement with the empirical relationship. Thus it appears that the relationship can be applied directly to obtain the air damping of plates under conditions similar to those encountered in this investigation. In more general cases, it appears that damping measurements under atmospheric conditions can be extrapolated by using the functional relationship found to exist between the variables.

Apparent mass effects.— When the effects of pressure environment on the vibratory response of a system are considered, frequency considerations are also of interest. The vibratory object experiences not only forces which oppose the velocity (damping forces) but also forces proportional to the acceleration which effectively alter the mass as discussed in reference 3. To examine the importance of this effect, frequencies were measured for the 30-square-inch circular plate, while it was attached to both the high- and low-frequency



(a) Disks.

Figure 8.- Variation of air damping with parameter $\rho y/m$ for plates.



(b) Rectangles.

Figure 8.- Concluded.

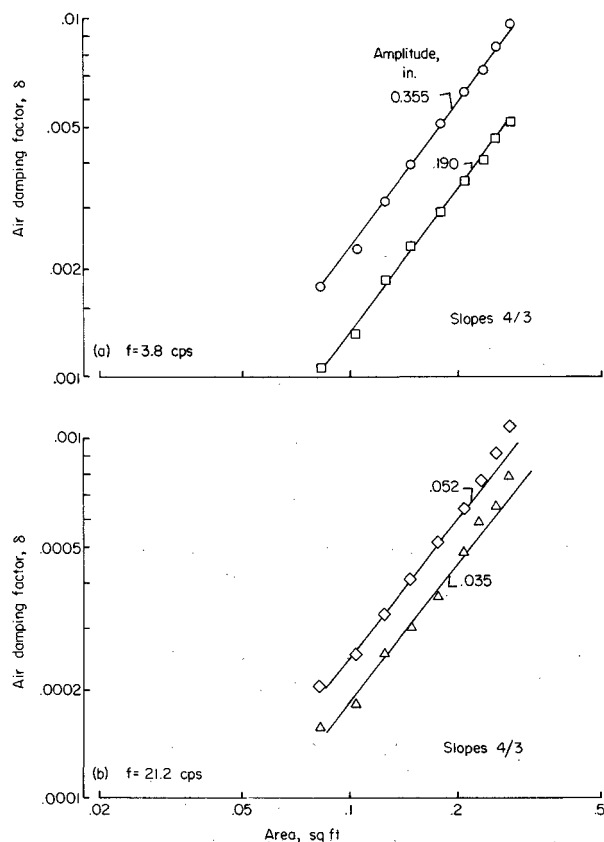


Figure 9.- Variation of air damping with area.

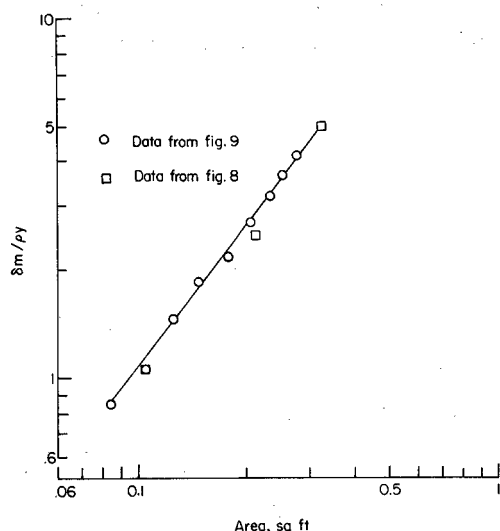


Figure 10.- Variation of parameter $\delta m / \rho y$ with area.

beams. The frequencies are shown in table II as a function of pressure and amplitude. In the low-frequency case a very slight increase (less than 0.3 percent) in frequency was noted as the pressure and hence apparent mass was decreased. No effect of pressure could be detected in the high-frequency case; thus, within the scope of this study apparent mass effects are considered to be negligible.

Damping of Three-Dimensional Models

Sphere.- The air damping experienced by the sphere with a projected surface area of 30 square inches is shown in figure 12. The decrement, presented as a function of pressure and amplitude, is essentially proportional to the square root of the pressure or density and is virtually independent of the amplitude. The independence of the air damping with amplitude is indicative of viscous damping forces as predicted by Lamb. (See ref. 3.) The magnitude of the theoretically predicted viscous force would yield the variation of damping with pressure shown by the dashed curve; these results are in very good agreement with the experimental data. The theoretical decrement

$$\delta = \frac{3\pi^2 \rho a^3 \left(\frac{1}{\beta a} + \frac{1}{\beta^2 a^2} \right)}{m} \quad (17)$$

appears to be quite adequate for the prediction of the damping.

Cylinder.- Similar results obtained for the cylinder are shown in figure 13 and are compared with the theory of Stokes for an infinite cylinder. Again, the decrement is proportional to the square root of the density and is in excellent agreement with the theory in the case of low amplitude. At high amplitudes, however, a discrepancy of

the damping with amplitude is noted possibly because of end effects or partial separation of the flow. However, the relationship

$$\delta = \frac{\pi^2 a^2 \rho l \left(\frac{2}{\beta a} + \frac{1}{\beta^2 a^2} \right)}{m} \quad (19)$$

is probably adequate for predicting the damping in most engineering applications. It should be noted that in the cases of the sphere and cylinder, no variation of frequency with pressure was noted throughout the pressure range examined.

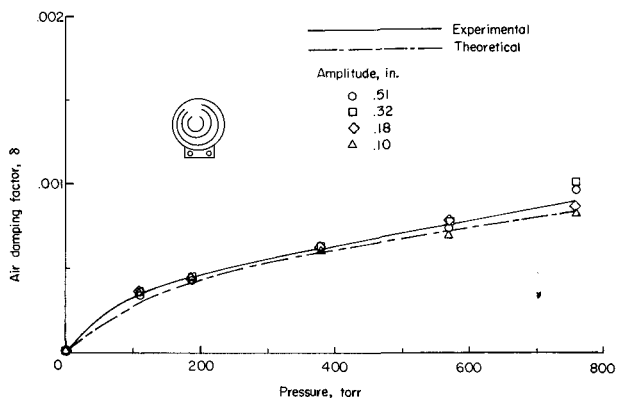


Figure 12.- Variation of air damping with pressure for the sphere. $f = 3.8$ cps.

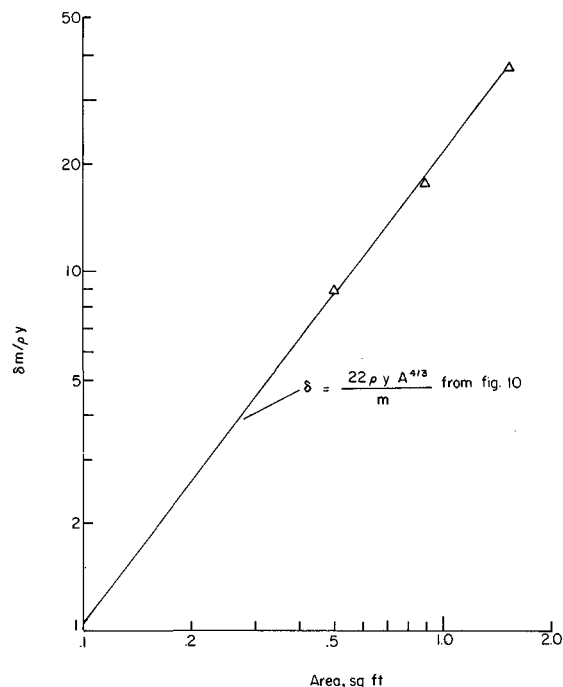


Figure 11.- Variation of parameter $\delta m / \rho y$ for large areas.

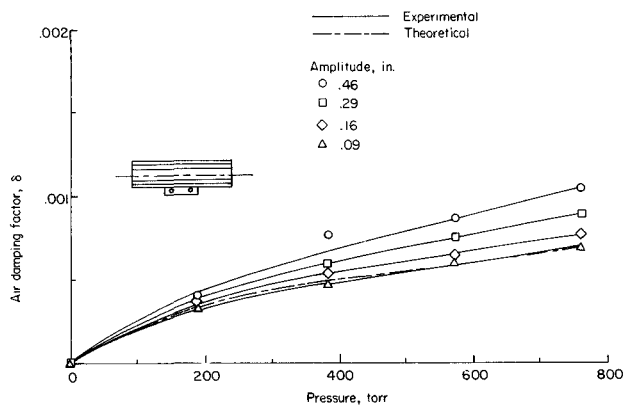


Figure 13.- Variation of air damping with pressure for the cylinder. $f = 3.8$ cps.

CONCLUSIONS

An investigation has been conducted to determine the air damping exhibited by rigid two- and three-dimensional shapes oscillating in a pressure environment ranging from 4×10^{-2} torr to 760 torr. Within the range of variables considered in this investigation, the following conclusions are noted:

1. For systems having a relatively large ratio of area to mass, the magnitude of the air damping may greatly exceed the damping attributed to all other sources. Values of air damping, an order of magnitude greater than the structural damping, were observed in these tests.

2. The damping factors associated with the two-dimensional plates exhibit a linear dependency on pressure and, except for relatively low amplitudes, a near-linear dependency on amplitude. Thus the damping forces are apparently proportional to the dynamic pressure.

3. For the plates, the damping is independent of shape and varies with the $4/3$ power of the area.

4. The empirical relationship which best describes the dependency of the air damping of the plates on the variables, air density ρ , amplitude y , area A , and mass m , is $\delta = K \frac{\rho y A^{4/3}}{m}$, where K is equal to 22 in U.S. customary units.

5. The damping factors associated with the sphere are essentially proportional to the square root of the density, independent of the vibratory amplitude, and in good agreement with available theory based on viscous damping forces.

6. At low amplitudes the cylinder exhibits damping factors in excellent agreement with those predicted by viscous theory. At higher amplitudes the damping exceeds theoretical predictions - possibly because of end effects or flow separation.

7. The response frequency is virtually unaffected by changes in pressure and amplitude; therefore, apparent mass effects are considered to be negligible.

Langley Research Center,
National Aeronautics and Space Administration,
Langley Station, Hampton, Va., December 9, 1964.

REFERENCES

1. Crandall, Stephen H.: On Scaling Laws for Material Damping. NASA TN D-1467, 1962.
2. Lazan, B. J.; and Goodman, L. E.: Material and Interface Damping. Data Analysis, Testing, and Methods of Control. Vol. 2 of Shock and Vibration Handbook, Cyril M. Harris and Charles E. Crede, eds., McGraw-Hill Book Co., Inc., 1961, pp. 36-1 - 36-46.
3. Lamb, Horace: Hydrodynamics. Sixth ed., Dover Pub., 1945.
4. Stokes, G. G.: On the Effect of Internal Friction of Fluids on the Motion of Pendulums. Trans. Cambridge Phil. Soc., vol. IX, pt. II, 1851, pp. 8-106.
5. Stuart, J. T.; and Woodgate, L.: Experimental Determination of the Aerodynamic Damping on a Vibrating Circular Cylinder. Rept. No. F.M. 1992, Brit. N.P.L. (Rept. No. 16,375, A.R.C.), Dec. 8, 1953.
6. Hubbard, Harvey H., and Houbolt, John C.: Vibration Induced by Acoustic Waves. Engineering Design and Environmental Conditions. Vol. 3 of Shock and Vibration Handbook, Cyril M. Harris and Charles E. Crede, eds., McGraw-Hill Book Co., Inc., c.1961, pp. 48-1 - 48-57.
7. Rayleigh, (Lord): The Theory of Sound. First Am. ed., vol. II, Dover Publ., 1945.
8. Baker, W. E.; and Allen, F. J.: The Damping of Transverse Vibrations of Thin Beams in Air. Rept. No. 1033, Ballistic Res. Labs., Aberdeen Proving Ground, Oct. 1957.
9. Thomson, William Tyrrell: Mechanical Vibrations. Second ed., Prentice-Hall, Inc., c.1953.
10. Keulegan, Garbis H.; and Carpenter, Lloyd H.: Forces on Cylinders and Plates in an Oscillating Fluid. Res. Paper 2857, Jour. Res. of Nat. Bur. Standards, vol. 60, no. 5, May 1958, pp. 423-440.

TABLE I.- INFORMATION PERTINENT TO MODELS AND TESTS CONDUCTED

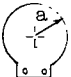
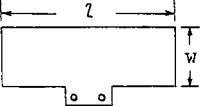
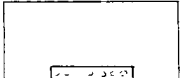
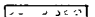


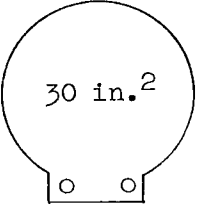
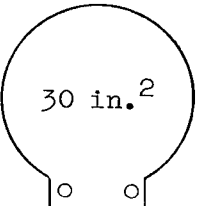
Model	Sketch of model	Configuration	Model description						Test conditions	
			l, in.	w, in.	a, in.	t, in.	Projected area, sq in.	Material	f, cps	p, torr
A		Circular plates	----	----	2.185	0.120	15	Steel	3.8	4×10^{-2} to 760
B		Circular plates	----	----	3.09	.156	30	Aluminum	3.8 and 21.2	4×10^{-2} to 760
C		Circular plates	----	----	3.735	.120	45	Aluminum	3.8	4×10^{-2} to 760
D		Rectangular plates	4	3	----	.120	12	Steel	3.8 and 21.2	4×10^{-2} to 760
E		Rectangular plates	5	3	----	.120	15	Steel	3.8 and 21.2	4×10^{-2} to 760
F		Rectangular plates	6	3	----	.120	18	Aluminum	3.8 and 21.2	4×10^{-2} to 760
G		Rectangular plates	7	3	----	.120	21	Aluminum	3.8 and 21.2	4×10^{-2} to 760
H		Rectangular plates	8.5	3	----	.120	25.5	Aluminum	3.8 and 21.2	4×10^{-2} to 760
I		Rectangular plates	10	3	----	.156	30	Aluminum	3.8 and 21.2	4×10^{-2} to 760
J		Rectangular plates	11	3	----	.120	33	Aluminum	3.8 and 21.2	4×10^{-2} to 760
K		Rectangular plates	12	3	----	.120	36	Aluminum	3.8 and 21.2	4×10^{-2} to 760
L		Rectangular plates	13	3	----	.120	39	Aluminum	3.8 and 21.2	4×10^{-2} to 760
M		Rectangular plates	10	4.5	----	.120	45	Aluminum	3.8 and 21.2	4×10^{-2} to 760
N		Rectangular plates	12.5	7.5	----	.250	93.8	Steel	3.8	760
O		Rectangular plates	16	9.5	----	.250	152.0	Steel	3.8	760
P		Rectangular plates	20	12	----	.250	240	Aluminum	3.8	760
Q		Sphere	----	----	3.09	.120	30	Plastic	3.8	4×10^{-2} to 760
R		Cylinder	10	----	1.50	.120	30	Plastic	3.8	4×10^{-2} to 760

TABLE II.- EFFECT OF PRESSURE ON FREQUENCY

Configuration	Amplitude	Frequencies for pressures of -			
		760 torr	382 torr	189 torr	0.04 torr
 30 in. ²	0.514	3.767	3.767	3.770	3.771
	.323	3.763	3.768	3.770	3.771
	.181	3.763	3.768	3.770	3.772
	.103	3.764	3.768	3.771	3.772
 30 in. ²	0.024	21.23	21.20	21.17	20.99
	.014	21.23	21.29	21.28	21.21
	.010	21.29	21.22	21.26	21.15
	.008	21.29	21.26	21.20	21.26

ME
2/6/85

"The aeronautical and space activities of the United States shall be conducted so as to contribute . . . to the expansion of human knowledge of phenomena in the atmosphere and space. The Administration shall provide for the widest practicable and appropriate dissemination of information concerning its activities and the results thereof."

—NATIONAL AERONAUTICS AND SPACE ACT OF 1958

NASA SCIENTIFIC AND TECHNICAL PUBLICATIONS

TECHNICAL REPORTS: Scientific and technical information considered important, complete, and a lasting contribution to existing knowledge.

TECHNICAL NOTES: Information less broad in scope but nevertheless of importance as a contribution to existing knowledge.

TECHNICAL MEMORANDUMS: Information receiving limited distribution because of preliminary data, security classification, or other reasons.

CONTRACTOR REPORTS: Technical information generated in connection with a NASA contract or grant and released under NASA auspices.

TECHNICAL TRANSLATIONS: Information published in a foreign language considered to merit NASA distribution in English.

TECHNICAL REPRINTS: Information derived from NASA activities and initially published in the form of journal articles.

SPECIAL PUBLICATIONS: Information derived from or of value to NASA activities but not necessarily reporting the results of individual NASA-programmed scientific efforts. Publications include conference proceedings, monographs, data compilations, handbooks, sourcebooks, and special bibliographies.

Details on the availability of these publications may be obtained from:

SCIENTIFIC AND TECHNICAL INFORMATION DIVISION
NATIONAL AERONAUTICS AND SPACE ADMINISTRATION
Washington, D.C. 20546